

## Electronic Supplementary Information

# Electron Belt-to- $\sigma$ -Hole Switch of Noncovalently Bound Iodine(I) Atoms in Dithiocarbamate Metal Complexes

Lev E. Zelenkov,<sup>1,2</sup> Anastasiya A. Eliseeva,<sup>1</sup> Sergey V. Baykov,<sup>1</sup> Vitalii V. Suslonov,<sup>1</sup> Bartomeu Galmés,<sup>3</sup> Antonio Frontera,<sup>3</sup> Vadim Yu. Kukushkin,<sup>1,4</sup> Daniil M. Ivanov,\*<sup>1</sup> Nadezhda A. Bokach,\*<sup>1</sup>

<sup>1</sup>*Institute of Chemistry, Saint Petersburg State University, Universitetskaya Nab. 7/9,  
Saint Petersburg, 199034 Russian Federation*

<sup>2</sup>*ITMO University, Saint Petersburg, 191002 Russian Federation*

<sup>3</sup>*Department of Chemistry, Universitat de les Illes Balears, Crta de Valldemossa km 7.5, 07122 Palma de  
Mallorca (Baleares), Spain*

<sup>4</sup>*Laboratory of Crystal Engineering of Functional Materials, South Ural State University, 76, Lenin Av.,  
Chelyabinsk, 454080 Russian Federation*

## Table of Contents

Experimental Section .....	3
Applications of dithiocarbamates .....	5
Crystallographic data.....	6
Results of Hirshfeld surface analysis.....	8
Noncovalent interactions .....	9
Parameters of halogen bonds involving dithiocarbamate ligands.....	13
Theoretical studies.....	15
Electron localization function projections for (1–4)·2FIB.....	18
References .....	19

## Experimental Section

**1. Materials and instrumentation.** Solvents were obtained from commercial sources and used as received. Et<sub>2</sub>NCS<sub>2</sub>Na trihydrate is commercially available and was recrystallized before use by adding Et<sub>2</sub>O to hot ethanol solution followed by refrigerator cooling ( $-10\text{ }^{\circ}\text{C}$ ) and filtration. Metal complexes **1–2** are commercially available and were purified by Soxhlet extraction followed by recrystallisation from CHCl<sub>3</sub>. Metal complexes **3–4** was synthesized accordingly to the modified published procedures:<sup>1, 2</sup> to a stirred solution of Et<sub>2</sub>NCS<sub>2</sub>Na trihydrate (100 mg, 0.443 mmol) in mixed solvent (EtOH:H<sub>2</sub>O 1:1, v/v; 7 mL) was added dropwise over a period of 3 min a solution of K<sub>2</sub>MCl<sub>4</sub> (0.220 mmol, M = Pd, Pt) in H<sub>2</sub>O (10 mL). Immediately formed precipitation was stirred for additional 20 min and then was filtered off with deionized H<sub>2</sub>O washing (3 x 15 mL). The precipitation was dried and stored over P<sub>4</sub>O<sub>10</sub>.

**2. Crystal growth.** Co-crystallization of **1–4** with FIB. A mixture of 0.250 mmol of any one of **1–4** and 0.504 mmol of FIB (25.7 mg) was dissolved in dichloromethane (2.5 mL), whereupon the formed solution was left to stand at room temperature for slow evaporation. Crystals of **(1–4)·2FIB** suitable for X-ray diffraction analysis were obtained after 2–5 d.

**3. X-ray structure determinations.** The X-ray diffraction experiments were carried out on the Rigaku “XtaLAB SuperNova” diffractometer using monochromated CuK $\alpha$  radiation. The crystals were thermostated at 100 K at all experiments. The structures were solved within Olex2<sup>3</sup> GUI package by the ShelXT<sup>4</sup> using Intrinsic Phasing method and refined by the ShelXL<sup>5</sup> refinement package using least square minimization. Since the betta parameter for all structures is close to the 90° edge, in order to maintain uniformity, the unit cell parameters of the platinum and palladium dithiocarbamates were converted to an unreduced cell using WinGX<sup>6</sup> program. Empirical absorption correction was applied in CrysAlisPro (Rigaku Oxford Diffraction, 2019) program complex using spherical harmonics, implemented in SCALE3 ABSPACK scaling algorithm. Supplementary crystallographic data for this paper have been deposited at Cambridge

Crystallographic Data Centre (CCDC 2044963–2044966) and can be obtained free of charge via [www.ccdc.cam.ac.uk/structures](http://www.ccdc.cam.ac.uk/structures).

**4. Details of Hirshfeld surface analysis.** The Hirshfeld surface analysis was carried out using the CrystalExplorer program.<sup>7-10</sup> The contact distances ( $d_{\text{norm}}$ ), based on  $R_{\text{vdW}}$ ,<sup>11</sup> were mapped on the Hirshfeld surfaces. In the color scale, the negative values of  $d_{\text{norm}}$  were visualized by red color indicating the contacts shorter than  $\Sigma_{\text{vdW}}$ . The values represented in white color denote the intermolecular distances close to the contacts with  $d_{\text{norm}}$  equal to zero. The contacts longer than  $\Sigma_{\text{vdW}}$  with positive  $d_{\text{norm}}$  values were colored with blue.

**5. Computational details.** The calculations of the dimers shown in **Figures 8–9** were performed at the DFT level of theory using PBE0 functional,<sup>12</sup> the def2-TZVP basis set<sup>13</sup> and the D3 dispersion correction<sup>14</sup> with the help of the Turbomole 7.0 program package.<sup>15</sup> The topological analysis of the electron density distribution has been analyzed with the help of the atoms in molecules (QTAIM) method developed by Bader<sup>16</sup> as well as noncovalent interaction plot (NCIPlot)<sup>17, 18</sup> by using the AIMAll program.<sup>19</sup> The estimation of the individual XB energies was carried out using the QTAIM method and the V(r) predictor as recently proposed in the literature.<sup>20</sup> The electron localization function (ELF) projections along the planes as well as ELF, electron density, and electrostatic potential (calculated with LIBRETA<sup>21</sup>) projections along the bond paths were plotted in Multiwfn 3.8.<sup>22</sup> The MEP surfaces and NBO analysis<sup>23</sup> were computed at the PBE0-D3/def2-TZVP level of theory by means of the Gaussian-16 program.<sup>24</sup> The MEP plots of **Figures S1–S2** were represented using the 0.001 a.u. isosurface.

## Applications of dithiocarbamates

The homoleptic dithiocarbamates [ $M(S_2CNR_2)_2$ ] (**Figure 2**; R = Et) found their applications in medicine,<sup>25-45</sup> photovoltaics,<sup>46-48</sup> syntheses of metal sulfides<sup>39, 48-56</sup> and polinuclear coordination compounds;<sup>57-78</sup> these metal complexes are useful as luminescent materials<sup>42-45, 79-81</sup> and chemical sensors.<sup>42, 48, 50, 82, 83</sup>

# Crystallographic data

**Table S1.** Crystallographic data and structure refinement for (**1–4**)·2FIB.

Identification code	<b>1</b> ·2FIB	<b>2</b> ·2FIB	<b>3</b> ·2FIB	<b>4</b> ·2FIB
CCDC number	2044963	2044964	2044966	2044965
Empirical formula	C <sub>22</sub> H <sub>20</sub> CuF <sub>6</sub> I <sub>6</sub> N <sub>2</sub> S <sub>4</sub>	C <sub>22</sub> H <sub>20</sub> F <sub>6</sub> I <sub>6</sub> N <sub>2</sub> NiS <sub>4</sub>	C <sub>22</sub> H <sub>20</sub> F <sub>6</sub> I <sub>6</sub> N <sub>2</sub> PdS <sub>4</sub>	C <sub>22</sub> H <sub>20</sub> F <sub>6</sub> I <sub>6</sub> N <sub>2</sub> PtS <sub>4</sub>
Formula weight	1379.58	1374.75	1422.44	1511.13
Temperature, K		100(2)		
Crystal system	triclinic	triclinic	triclinic	triclinic
Space group	P-1	P-1	P-1	P-1
a, Å	8.6789(3)	8.6870(2)	8.6378(2)	8.6611(2)
b, Å	9.4436(3)	9.4313(2)	9.5068(3)	9.6024(2)
c, Å	12.4868(2)	12.2577(2)	12.3335(3)	12.1690(2)
α, °	107.682(2)	106.930(2)	107.763(3)	107.288(2)
β, °	90.978(2)	91.1590(10)	89.773(2)	89.909(2)
γ, °	114.817(3)	113.553(2)	113.626(3)	113.544(2)
Volume, Å <sup>3</sup>	872.57(5)	869.96(3)	875.50(5)	877.93(3)
Z	1	1	1	1
ρ <sub>calc</sub> , g·cm <sup>-3</sup>	2.625	2.624	2.698	2.858
μ, mm <sup>-1</sup>	45.254	45.309	48.499	51.576
F(000)	631.0	630.0	648.0	680.0
Crystal size, mm <sup>3</sup>	0.17 × 0.15 × 0.14	0.2 × 0.18 × 0.15	0.15 × 0.14 × 0.12	0.20 × 0.16 × 0.14
Radiation	CuKα (λ = 1.54184)			
2Θ range for data collection, °	7.536 to 134.96	7.632 to 124.91	7.596 to 140.984	7.678 to 140.876
Index ranges	−10 ≤ h ≤ 10, −11 ≤ k ≤ 11, −14 ≤ l ≤ 14	−9 ≤ h ≤ 9, −10 ≤ k ≤ 10, −14 ≤ l ≤ 13	−10 ≤ h ≤ 10, −11 ≤ k ≤ 11, −15 ≤ l ≤ 15	−10 ≤ h ≤ 10, −11 ≤ k ≤ 11, −14 ≤ l ≤ 14
Reflections collected	14534	14447	16237	7998
Independent reflections	3146 [R <sub>int</sub> = 0.0581, R <sub>sigma</sub> = 0.0386]	2765 [R <sub>int</sub> = 0.0537, R <sub>sigma</sub> = 0.0261]	3340 [R <sub>int</sub> = 0.0499, R <sub>sigma</sub> = 0.0352]	3352 [R <sub>int</sub> = 0.0448, R <sub>sigma</sub> = 0.0529]
Data/restraints/parameters	3146/0/189	2765/0/189	3340/0/189	3352/0/183
Goodness-of-fit on F <sup>2</sup>	1.032	1.096	1.072	1.011
Final R indexes [I ≥ 2σ(I)]	R <sub>1</sub> = 0.0346, wR <sub>2</sub> = 0.0882	R <sub>1</sub> = 0.0366, wR <sub>2</sub> = 0.0985	R <sub>1</sub> = 0.0352, wR <sub>2</sub> = 0.0916	R <sub>1</sub> = 0.0348, wR <sub>2</sub> = 0.0842
Final R indexes [all data]	R <sub>1</sub> = 0.0386, wR <sub>2</sub> = 0.0899	R <sub>1</sub> = 0.0371, wR <sub>2</sub> = 0.0990	R <sub>1</sub> = 0.0383, wR <sub>2</sub> = 0.0941	R <sub>1</sub> = 0.0381, wR <sub>2</sub> = 0.0871
Largest diff. peak/hole, e·Å <sup>-3</sup>	2.41/−1.00	1.73/−2.57	1.27/−2.17	1.70/−1.86

**Table S2.** Geometrical parameters of the chelated S1C1S2 rings in the metal complexes in their co-crystals.

M	Cu	Ni	Pd	Pt
$d(M1-S1)$ , Å	2.2988(12)	2.2066(14)	2.3280(13)	2.3276(14)
$d(M1-S2)$ , Å	2.3164(13)	2.2131(14)	2.3325(13)	2.3270(15)
$d(S1-C1)$ , Å	1.732(5)	1.729(6)	1.741(6)	1.718(6)
$d(S2-C1)$ , Å	1.720(5)	1.723(6)	1.738(6)	1.739(6)
$\angle(S1-C1-S2)$ , °	113.4(3)	109.4(3)	110.0(3)	110.1(3)
$\angle(S1-M1-S2)$ , °	77.36(4)	79.22(5)	75.35(5)	74.99(5)
$\angle(M1-S1-C1)$ , °	84.74(16)	85.7(2)	87.4(2)	87.7(2)
$\angle(M1-S2-C1)$ , °	84.46(18)	85.6(2)	87.3(2)	87.7(2)

## Results of Hirshfeld surface analysis

**Table S3.** Results of Hirshfeld surface analysis for the X-ray diffraction structures of the co-crystals.

Structure	Contributions of different intermolecular contacts to the molecular Hirshfeld surface*
<b>1·2FIB</b>	I···Cu 2.9%, I···S 8.6%, I···C 1.2%, I···H 12.8%, S···H 23.4%, F···H 21.1%, N···H 1.0%, C···H 10.0%, H···H 18.0%
<b>2·2FIB</b>	I···Ni 2.9%, I···S 9.1%, I···C 1.0%, I···H 13.6%, S···H 21.8%, F···H 22.0%, N···H 1.0%, C···H 9.9%, H···H 17.8%
<b>3·2FIB</b>	I···Pd 3.1%, I···S 8.6%, I···H 13.7%, S···H 23.2%, F···H 22.3%, C···H 9.5%, H···H 16.5%
<b>4·2FIB</b>	I···Pt 3.3%, I···S 9.0%, I···H 14.2%, S···H 22.6%, F···H 22.5%, C···H 9.5%, H···H 15.8%

\*The contributions of all other intermolecular contacts do not exceed 1%.

## Noncovalent interactions

**Table S4.** Parameters of the C–I…S and C–I…M/M…I–C short contacts in the co-crystals.

Parameter	1·2FIB	2·2FIB	3·2FIB	4·2FIB
$d(I1S\cdots M1)$ , Å	3.3924(3)	3.3388(4)	3.3732(4)	3.3351(4)
$R_{\text{Bondi}}$	1.00	0.92	0.93	0.89
$\angle(C1S-I1S\cdots M1)$ , °	137.06(16)	149.1(2)	153.0(2)	160.1(2)
$d(I1S\cdots S1)$ , Å	3.4523(11)	3.6826(13)	3.8447(12)	4.0172(14)
$R_{\text{Bondi}}$	0.91	0.97	1.02	1.06
$\angle(C1S-I1S\cdots S1)$ , °	175.89(18)	174.15(19)	169.18(19)	164.0(2)
$d(I1S\cdots S2)$ , Å	3.8775(13)	3.7383(15)	3.7221(14)	3.6931(16)
$R_{\text{Bondi}}$	1.03	0.99	0.98	0.98
$\angle(C1S-I1S\cdots S2)$ , °	133.30(15)	140.2(2)	143.7(2)	145.4(2)
$d(I2S\cdots S2)$ , Å	3.3994(12)	3.4089(15)	3.3929(13)	3.4161(15)
$R_{\text{Bondi}}$	0.90	0.90	0.90	0.90
$\angle(C3S-I2S\cdots S2)$ , °	169.01(13)	166.25(17)	165.12(14)	163.87(16)

<sup>a</sup>  $R_{\text{Bondi}}^{84} = d/\Sigma_{\text{vdW}}$ ;  $\Sigma_{\text{vdW}}(\text{I, Cu}) = 3.38$  Å,  $\Sigma_{\text{vdW}}(\text{I, Ni}) = 3.61$  Å,  $\Sigma_{\text{vdW}}(\text{I, Pd}) = 3.61$  Å,  $\Sigma_{\text{vdW}}(\text{I, Pt}) = 3.73$  Å,  $\Sigma_{\text{vdW}}(\text{I, S}) = 3.78$  Å.

**Table S5.** Previously reported R–I…M (M = Ni, Pd, Pt) halogen bonding.

Structure	$d(\text{I}\cdots\text{M})$ , Å	$R_{IM}$	$\angle(R-\text{I}\cdots\text{M})$ , °	Refs.
<b>M = Ni</b>				
2·2FIB	3.3388(4)	0.92	149.1(2)	<i>This work</i>
AMIJAJ	3.4702(17)	0.96	177.8(4)	<sup>85, 86</sup>
<b>M = Pd</b>				
LOFXAH	3.0953(6)	0.86	178.871(12)	<sup>87</sup>
	3.1021(6)	0.86	178.192(11)	
3·2FIB	3.3732(4)	0.93	153.0(2)	<i>This work</i>
AMIJIR	3.4978(3)	0.97	177.57(7)	<sup>85, 88</sup>
LIHMEX	3.5125(4)	0.97	164.94(15)	<sup>88</sup>
IJIFEP	3.5433(4)	0.98	170.61(9)	<sup>89</sup>
IJIDUD	3.6422(4)	1.01	167.68(13)	<sup>89</sup>
<b>M = Pt</b>				
PIDRIE	2.8198(3)	0.76	177.533(15)	<sup>90</sup>
	2.8260(3)	0.76	177.248(14)	
DUGJUK	2.895(1)	0.78	179.42(4)	<sup>91</sup>
DEJHEF	2.906(2)	0.78	176.91(4)	<sup>91</sup>
	2.968(2)	0.80	177.72(6)	<sup>92</sup>
XUVXUK	3.0891(4)	0.83	167.8(2)	<sup>93</sup>
	3.0979(4)	0.83	177.60(17)	
	3.1264(4)	0.84	175.99(18)	
	3.1379(4)	0.84	167.5(2)	

XUVXOE	3.1933(3)	0.86	174.11(10)	<sup>93</sup>
XUVYAR	3.2494(4)	0.87	174.28(16)	<sup>93</sup>
<b>4·2FIB</b>	<b>3.3351(4)</b>	<b>0.89</b>	<b>160.1(2)</b>	<i>This work</i>
UKELAZ	3.4023(5)	0.91	172.7(2)	<sup>94</sup>
UKEKOM	3.4276(5)	0.92	164.80(17)	<sup>94</sup>
UKEKIG	3.4389(5)	0.92	169.8(3)	<sup>94</sup>
ROZZUE	3.4504(3)	0.93	168.75(10)	<sup>95</sup>
AMIJEN	3.4666(4)	0.93	177.14(13)	<sup>85, 88</sup>
XUVYEV	3.4743(8)	0.93	168.6(2)	<sup>93</sup>
UKAWOU	3.7060(7)	0.99	158.4(2)	<sup>94</sup>

*Comments to semicoordinative/XB I···(S–Cu) contact (section 2.2.1).* Complexes [Cu<sup>II</sup>(S<sub>2</sub>CNR<sub>2</sub>)<sub>2</sub>] are known<sup>96–98</sup> as weak Cu-centered electrophiles, which according to the EPR data can coordinate two pyridines.<sup>96</sup> These metal complexes tend to dimerize or polymerize through a pair of Cu<sup>II</sup>···S semicoordinative interactions (**Figure 6J**).<sup>28, 67, 99–102</sup> We assume that these data, together with performed theoretical calculations (**section 3**) confirm the semicoordinative nature of the Cu<sup>II</sup>···I–C contact in the structure of **1·2FIB** even considering that  $\angle(\text{Cu}^{\text{II}}\cdots\text{I–C})$  137.06(16) $^\circ$  is substantially larger than 90 $^\circ$ .

The nucleophilic nature of the I1S atom in the Cu1···I1S–C1S contact is not unprecedented. Similar interaction of iodine atom via its electron belt has been observed in CSD structure OJIJC, where type II iodine···iodine contact C43–I5···I2–C33 between FIBs was identified. In OJIJC structure, the angle around the nucleophilic I2 atom (135.83(8) $^\circ$ ) is close to  $\angle(\text{Cu}^{\text{II}}\cdots\text{I–C})$  137.06(16) $^\circ$ , which we observed in the structure of **1·2FIB**. This comparison provides certain evidences favoring the nucleophilic role of FIB toward the copper(II) center.

*Comments to the C–I···Ni halogen bonding (section 2.2.2).* Our observation of nickel(II)-involving XB correlates with the previously reported C–H···Ni<sup>II</sup> hydrogen bonding in the structures of various nickel(II) dithiocarbamates (**Figure 7L**).<sup>47, 103–109</sup>

*Comments to the C–I···Pd halogen bonding (section 2.2.3.).* Similar to the nickel(II) center in the structure of **2·2FIB**, the palladium(II) atom in **3·2FIB** can also form both Pd<sup>II</sup>···I semicoordination bond and I···Pd<sup>II</sup> XB (**Table 4**). The structure of [Pd( $\mu$ -SCH<sub>2</sub>CO<sub>2</sub>Me)<sub>2</sub>]<sub>8</sub>·I<sub>2</sub><sup>87</sup>

(LOFXAH) demonstrates the shortest I···Pd<sup>II</sup> XB (3.0953(6) Å and 3.1021(6) Å) and the formation of the strong XB is accounted for by the deep σ<sub>h</sub> of I<sub>2</sub> and the inclusion character of the co-crystal. The longest I···Pd<sup>II</sup> XB has been reported for *trans*-[PdCl<sub>2</sub>(NCNMe<sub>2</sub>)<sub>2</sub>]·2CHI<sub>3</sub> (3.5125(4) Å) (LIHMEX).<sup>88</sup> A slightly shorter I···Pd<sup>II</sup> XB can be found in [Fe(2-iodopyrazine)(H<sub>2</sub>O)M<sup>II</sup>(CN)<sub>4</sub>] (M = Pd) MOF (3.4978(3) Å) (AMIJIR).<sup>85</sup> In a recent study by one of us,<sup>89</sup> the half-lantern complexes *trans*-(E,N)-[Pd(ppz)(μ-E<sup>◦</sup>N)]<sub>2</sub> (E<sup>◦</sup>N is a deprotonated 2-substituted pyridine; E = S, Se; Hppz = 1-phenylpyrazole) were cocrystallized with 1,4-diiidotetrafluorobenzene to give *trans*-(E,N)-[Pd(ppz)(μ-E<sup>◦</sup>N)]<sub>2</sub>·2(1,4-diiidotetrafluorobenzene) (IJIFEP and IJIDUD). These two co-crystals are built by the joint action of I···Pd (3.6422(4) Å, E = S; 3.5433(4) Å, E = Se) and I···E XBs, thus furnishing clusters bearing the Pd<sup>II</sup><sub>2</sub>···I(arene<sup>F</sup>)I···E[@Pd<sup>II</sup><sub>2</sub>] linkages.

Notably, MOF is isostructural with previously mentioned nickel(II)-containing analog. Again, in **3**·2FIB, the C–I···Pd metal-involving XB (3.3732(4) Å) is shorter than in this MOF as well as in *trans*-[PdCl<sub>2</sub>(NCNMe<sub>2</sub>)<sub>2</sub>]·2CHI<sub>3</sub>, which confirms the increased nucleophilicity of metal center in the dithiocarbamate complex.

*Comments to the C–I···Pt halogen bonding (section 2.2.4).* Van Koten et al.<sup>90-92, 110</sup> reported the platinum(II) complex-diiodine adducts exhibiting short I–I···Pt<sup>II</sup> XB distances (2.8198(3)–2.968(2) Å; PIDRIE, DUGJUK, and DEJHEF; **Table 4**); this XB is so strong that it can be treated as coordinative XB.<sup>111</sup> The next strong contacts were observed in the co-crystals of the half-lantern complexes [{Pt(C<sup>◦</sup>N)(μ-S<sup>◦</sup>N)}<sub>2</sub>] (C<sup>◦</sup>N cyclometalated 2-Ph-benzothiazole; S<sup>◦</sup>N 2-SH-substituted N-heterocycles) with 1,4-diiidotetrafluorobenzene and 1,1'-I<sub>2</sub>-C<sub>6</sub>F<sub>4</sub>-C<sub>6</sub>F<sub>4</sub> (XUVXUK, XUVXOE, and XUVYAR), where metal centers exhibit an increased nucleophilicity toward XB donor.<sup>93</sup> Much weaker C–I···Pt<sup>II</sup> XB were identified by us<sup>94</sup> in *trans*-[PtCl<sub>2</sub>(NCNMe<sub>2</sub>)<sub>2</sub>]·2CHI<sub>3</sub> (UKEKIG, 3.4389(5) Å), *trans*-[PtCl<sub>2</sub>(NCNMe<sub>2</sub>)<sub>2</sub>]·0.5CHCl<sub>3</sub>·1.5CHI<sub>3</sub> (UKEKOM, 3.4276(5) Å), *trans*-[PtBr<sub>2</sub>(NCNMe<sub>2</sub>)<sub>2</sub>]·2CHI<sub>3</sub> (UKELAZ, 3.4023(5) Å), and the weakest one in *trans*-[PtCl<sub>2</sub>(NCN(CH<sub>2</sub>)<sub>5</sub>)<sub>2</sub>]·2CHI<sub>3</sub> (UKAWOU, 3.7060(7) Å) as a part of the

three-center bifurcated C–I···(Cl–Pt<sup>II</sup>) XB. The third example of [Fe(2-iodopyrazine)(H<sub>2</sub>O)M<sup>II</sup>(CN)<sub>4</sub>] MOF (AMIJEN),<sup>85</sup> where M = Pt, is also isostructural with the Ni and Pd analogs and demonstrates the same C–I···Pt<sup>II</sup> XB (3.4666(4) Å). FIB is also known<sup>95</sup> to form the C–I···Pt<sup>II</sup> XB in the co-crystal [Pt(acac)<sub>2</sub>]·2FIB (3.4077(3) Å).

## Parameters of halogen bonds involving dithiocarbamate ligands

**Table S6.** Parameters of NM–X···S (NM – any nonmetal; X = Cl, Br, I) XBs with dithiocarbamate ligands found in CCDC literature data.  $d(X\cdots S)$  distances are fixed as less than  $\Sigma_{vdW}$ , and  $\angle(NM-X\cdots S)$  are set between 150 and 180 degrees. Only non-disordered moieties, structures with R ≤ 10% are under consideration.

Structure	M	NM–X···S	$d(X\cdots S)$ , Å	$R_{XS}^*$	$\angle(NM-X\cdots S), ^\circ$
<b>X = Cl</b>					
BOMCEM	Sn <sup>IV</sup>	C31–Cl1···S3	3.516(2)	0.99	167.9(3)
BOSHAV	Nd <sup>III</sup>	C14–Cl2···S1	3.302(4)	0.93	167.6(3)
BOSHID	Eu <sup>III</sup>	C14–Cl1···S3	3.302(4)	0.93	169.0(3)
BOSHOJ	Eu <sup>III</sup>	C20–Cl2···S1	3.5276(14)	0.99	158.81(16)
DIFQIU	Pd <sup>II</sup>	C125–Cl7···S3	3.415(3)	0.96	167.8(4)
DUBBEJ	Ag <sup>I</sup>	C41–Cl1···S2	3.5362(17)	1.00	162.41(18)
DUHNUQ	Zn <sup>II</sup>	C33–Cl3···S2	3.3864(15)	0.95	159.53(13)
EJIXAW	Ni <sup>II</sup>	C23–Cl3···S2	3.352(2)	0.94	169.0(3)
GUVQOD	Zn <sup>II</sup>	C71–Cl5···S8	3.4580(16)	0.97	162.69(16)
HOWHOQ	Zn <sup>II</sup>	C9–Cl2···S1	3.317(3)	0.93	155.7(3)
	Zn <sup>II</sup>	C9–Cl3···S1	3.335(3)	0.94	168.1(3)
JOVQIX	Sn <sup>IV</sup>	C20–Cl2···S2	3.313(3)	0.93	167.9(3)
KENYOT	Pd <sup>II</sup>	C35–Cl1···S5	3.361(3)	0.95	175.3(4)
KIHZOS	Zn <sup>II</sup>	C1–Cl2···S1	3.475(4)	0.98	150.9(5)
KOXLER	Nd <sup>III</sup>	C40–Cl1···S5	3.381(5)	0.95	162.8(5)
MECBCR	Cr <sup>III</sup>	C20–Cl6···S1	3.514(2)	0.99	172.819(9)
MIKWAF	Sb <sup>III</sup>	C28–Cl2···S3	3.4954(14)	0.98	179.05(17)
MORTMN	Mn <sup>III</sup>	C16–Cl1···S2	3.382(3)	0.95	153.36(3)
MOWSIC	Au <sup>III</sup>	C41–Cl10···S6	3.547(6)	1.00	164.1(8)
MTCTAC10	Ta <sup>V</sup>	C7–Cl2···S4	3.5393(12)	1.00	166.758(6)
NAMFUF	Zn <sup>II</sup>	C14–Cl2···S4	3.4425(16)	0.97	158.89(14)
NICFAI	Sm <sup>III</sup>	C34–Cl3···S4	3.5143(11)	0.99	178.50(8)
NICFEM	Nd <sup>III</sup>	C34–Cl2···S6	3.5121(12)	0.99	178.66(11)
OCOWAG	Ru <sup>III</sup>	C16–Cl1···S3	3.5139(17)	0.99	157.16(16)
OCURUC	Bi <sup>III</sup>	C38–Cl6···S11	3.2868(18)	0.93	155.63(18)
OXIXEA	Zn <sup>II</sup>	C29–Cl1···S5	3.245(5)	0.91	172.8(6)
	Zn <sup>II</sup>	C30–Cl5···S1	3.297(5)	0.93	173.8(6)
OZEGAD	Cu <sup>I</sup>	C42–Cl3···S1	3.3488(10)	0.94	161.93(11)
PAZTMP10	Mo <sup>VI</sup>	C17–Cl4···S3	3.5378(9)	1.00	162.590(6)
QEWPPO	Os <sup>II</sup>	C24–Cl3···S1	3.1643(16)	0.89	150.0(3)
SURBOZ	Cu <sup>I</sup>	C54–Cl1···S2	3.5027(13)	0.99	161.00(14)
VIXRUQ	Au <sup>I</sup>	C15–Cl1···S1	3.515(5)	0.99	163.8(6)
XOCGED	Cu <sup>II</sup>	C11–Cl1···S2	3.443(8)	0.97	151.5(9)
XOLFIN	Mo <sup>IV</sup>	C36–Cl9···S5	3.498(4)	0.99	158.2(3)
XONHIS	Sn <sup>IV</sup>	C25–Cl1···S2	3.374(2)	0.95	168.2(2)
YERHOV	Cu <sup>II</sup>	C10–Cl2···S1	3.4364(11)	0.97	150.17(13)
ZUHGIU	La <sup>III</sup>	C31–Cl3···S6	3.4802(12)	0.98	160.06(13)
<b>X = Br</b>					
KUCBAL	V <sup>IV</sup>	C11–Br1···S3	3.530(6)	0.97	166.4(6)
MANTEA	Ru <sup>II</sup>	C4–Br1···S2	3.4064(19)	0.93	166.9(2)
NOQWEX	Sn <sup>IV</sup>	C18–Br2···S1	3.619(3)	0.99	152.69(14)
VOXQEN	Cu <sup>II</sup>	C6–Br1···S1	3.556(3)	0.97	174.2(3)
<b>X = I</b>					
ETCBFE	Fe <sup>IV</sup>	I2–I1···S6	3.628(3)	0.96	178.3553(17)
IATCNI	Ni <sup>II</sup>	As1–I1···S2	3.7551(4)	0.99	164.101(3)
MUJBIC	Co <sup>III</sup>	I2–I2···S2	3.1441(8)	0.83	175.42(2)
	Co <sup>III</sup>	I1–I1···S3	3.1484(9)	0.83	175.706(15)
ROHXAN	Ru <sup>II</sup>	I1–I1···S2	3.177(2)	0.84	172.34(5)

VIQFEH	Co <sup>III</sup>	I1–I1···S6	3.2281(12)	0.85	178.77(3)
${}^*R_{XS} = d(X \cdots S) / (R_{vdW}(X) + R_{vdW}(S))$					

## Theoretical studies

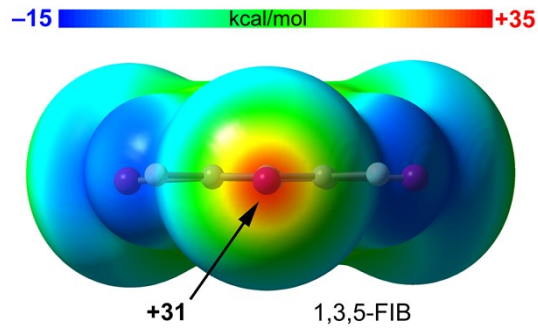


**Figure S1.** MEP surface (0.001 isosurface) of FIB at the PBE0-D3/def2-TZVP level of theory.

Energies in kcal/mol.

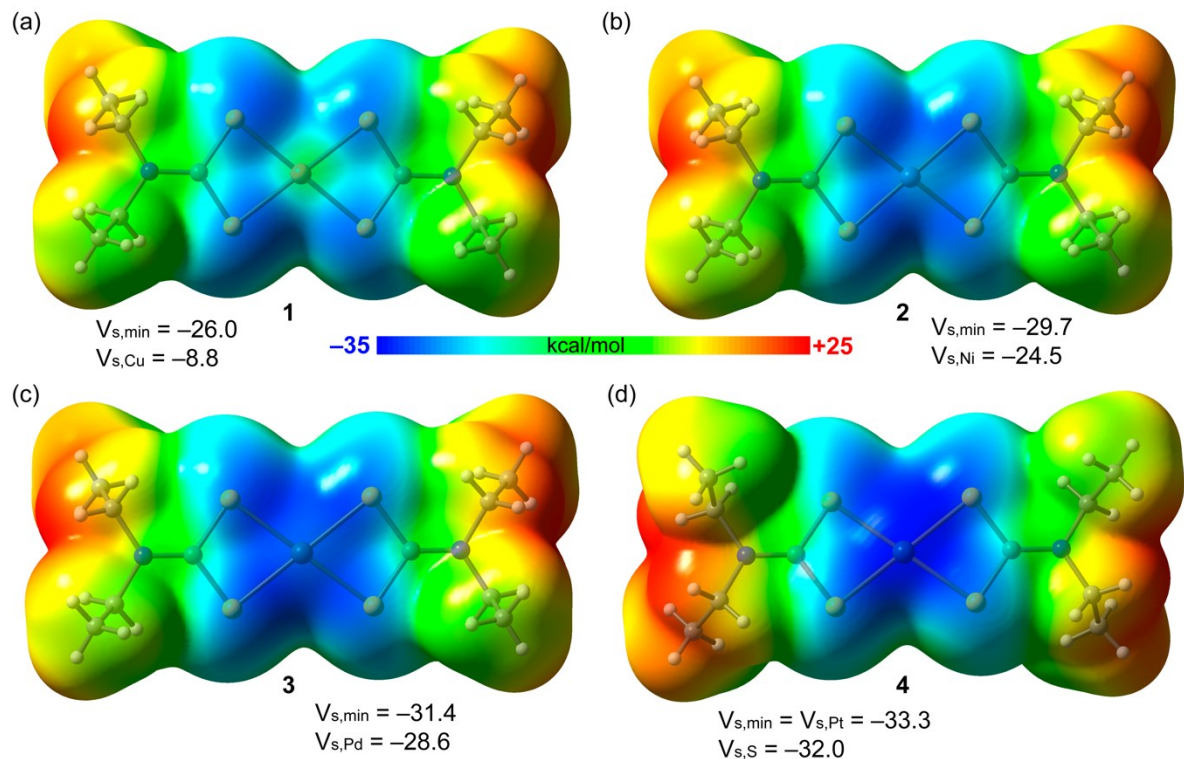


**Figure S2.** MEP surfaces (0.001 isosurface) of **1** (a), **2** (b), **3** (c), and **4** (d) at the PBE0-D3/def2-TZVP level of theory. Energies at S and M<sup>II</sup> centers are given in kcal/mol.

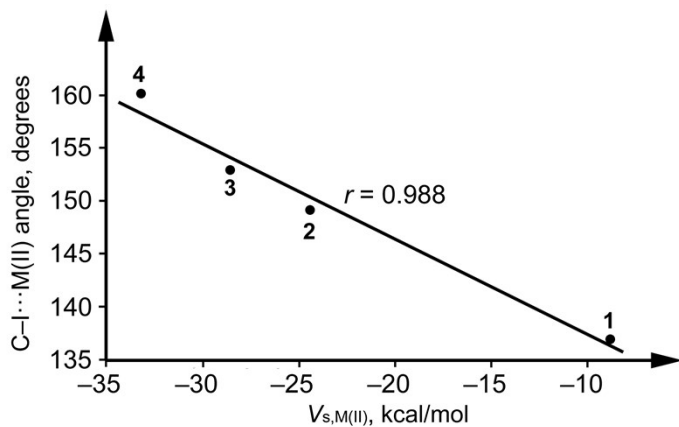


**Figure S3.** Regression plot of the C–I…M<sup>II</sup> angle of the XB interaction vs. the MEP value at the metal center ( $V_{s,M}^{II}$ ).

**Table S7.** QTAIM parameters ( $\rho$ ,  $\nabla^2\rho(r)$  and  $V(r)$  in a.u.) at the bond CP of I…S XB and I…H hydrogen bonds in the four model clusters reported herein (interactions depicted in **Figure 8**). Energy associated to each interaction based on the  $V_r$  parameter is also indicated (see computational methods)

Model cluster	CP	$\rho(r)$	$\nabla^2\rho(r)$	$V(r)$	E
<b>1·FIB</b>	I…S	0.0138	0.0348	-0.0068	3.32
	H…I	0.0057	0.0153	-0.0025	0.78
<b>2·FIB</b>	I…S	0.0139	0.0342	-0.0068	3.32
	H…I	0.0060	0.0155	-0.0026	0.82
<b>3·FIB</b>	I…S	0.0139	0.0338	-0.0068	3.32
	H…I	0.0059	0.0155	-0.0026	0.82
<b>4·FIB</b>	I…S	0.0144	0.0350	-0.0071	3.47
	H…I	0.0060	0.0159	-0.0027	0.85

**Table S8.** QTAIM parameters ( $\rho$ ,  $\nabla^2\rho(r)$  and  $V(r)$  in a.u.) at the bond CP of I…S XB and I…M XBs or semicoordination in the four model clusters reported herein (interactions depicted in **Figure 9**). Energy associated to each interaction based on the  $V_r$  parameter is also indicated (see computational methods)

Model cluster	CP	$\rho(r)$	$\nabla^2\rho(r)$	$V(r)$	E
<b>1·FIB</b>	I…S	0.0132	0.0342	-0.0066	3.22
	I…Cu	0.0118	0.0238	-0.0068	3.32
<b>2·FIB</b>	I…Ni	0.0133	0.0263	-0.0080	3.91
<b>3·FIB</b>	I…Pd	0.0188	0.0416	-0.0088	4.30
<b>4·FIB</b>	I…Pt	0.0188	0.0416	-0.0111	5.42



## Electron localization function projections for (1–4)·2FIB

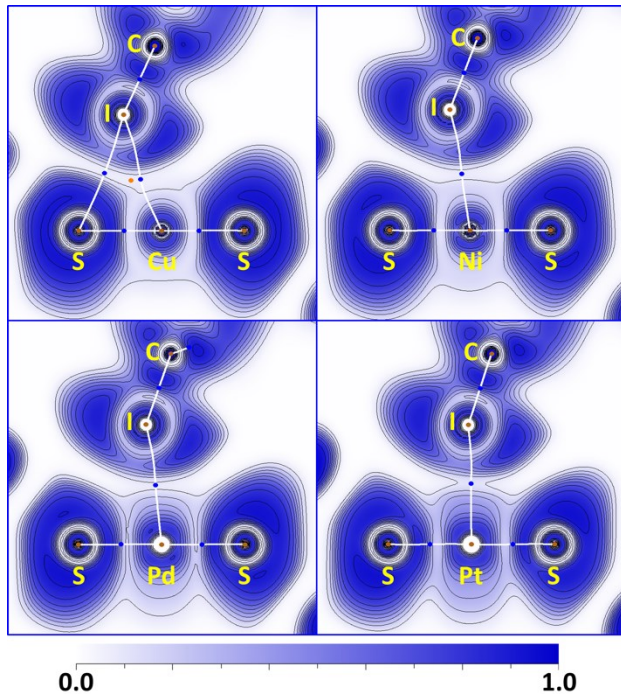


**Figure S4.** Electron localization function (ELF) projections with contour lines (0.1 step) along the S···S···I plane for the four model clusters. Bond (3, -1) critical points are blue, nuclear (3, -3) critical points are brown, ring (3, +1) critical points are orange, bond paths are white.

## References

1. F. Jian, F. Bei, P. Zhao, X. Wang, H. Fun and K. Chinnakali, Synthesis, Crystal Structure and Stability Studies of Dithiocarbamate Complexes of Some Transition Elements (M=Co, Ni, Pd), *Journal of Coordination Chemistry*, 2002, **55**, 429-437.
2. J. M. C. Alison and T. A. Stephenson, Metal complexes of sulphur ligands. Part III. Reaction of platinum(II)NN-dialkyldithiocarbamates, O-ethyl dithiocarbonate (xanthate), and OO'-diethyl dithiophosphate with tertiary phosphines, *Journal of the Chemical Society, Dalton Transactions*, 1973, DOI: 10.1039/DT9730000254, 254-263.
3. O. V. Dolomanov, L. J. Bourhis, R. J. Gildea, J. A. K. Howard and H. Puschmann, OLEX2: a complete structure solution, refinement and analysis program, *J. Appl. Crystallogr.*, 2009, **42**, 339-341.
4. G. Sheldrick, SHELXT - Integrated space-group and crystal-structure determination, *Acta Crystallographica Section A*, 2015, **71**, 3-8.
5. G. Sheldrick, Crystal structure refinement with SHELXL, *Acta Cryst. Sect. C*, 2015, **71**, 3-8.
6. L. Farrugia, WinGX and ORTEP for Windows: an update, *Journal of Applied Crystallography*, 2012, **45**, 849-854.
7. CrystalExplorer, <http://crystalexplorer.scb.uwa.edu.au>).
8. C. F. Mackenzie, P. R. Spackman, D. Jayatilaka and M. A. Spackman, CrystalExplorer model energies and energy frameworks: extension to metal coordination compounds, organic salts, solvates and open-shell systems, *IUCrJ*, 2017, **4**, 575-587.
9. J. J. McKinnon, D. Jayatilaka and M. A. Spackman, Towards quantitative analysis of intermolecular interactions with Hirshfeld surfaces, *Chem. Commun.*, 2007, DOI: 10.1039/B704980C, 3814-3816.
10. M. A. Spackman and D. Jayatilaka, Hirshfeld surface analysis, *CrystEngComm*, 2009, **11**, 19-32.
11. A. Bondi, Van der Waals Volumes and Radii, *J. Phys. Chem.*, 1964, **68**, 441–451.
12. C. Adamo and V. Barone, Toward reliable density functional methods without adjustable parameters: The PBE0 model, *J. Chem. Phys.*, 1999, **110**, 6158-6170.
13. F. Weigend, Accurate Coulomb-fitting basis sets for H to Rn, *Phys. Chem. Chem. Phys.*, 2006, **8**, 1057-1065.
14. S. Grimme, J. Antony, S. Ehrlich and H. Krieg, A consistent and accurate ab initio parametrization of density functional dispersion correction (DFT-D) for the 94 elements H-Pu, *J. Chem. Phys.*, 2010, **132**, 154104.
15. R. Ahlrichs, M. Bär, M. Häser, H. Horn and C. Kölmel, Electronic structure calculations on workstation computers: The program system turbomole, *Chem. Phys. Lett.*, 1989, **162**, 165-169.
16. R. F. W. Bader, A quantum theory of molecular structure and its applications, *Chem. Rev.*, 1991, **91**, 893-928.
17. E. R. Johnson, S. Keinan, P. Mori-Sánchez, J. Contreras-García, A. J. Cohen and W. Yang, Revealing Noncovalent Interactions, *J. Am. Chem. Soc.*, 2010, **132**, 6498-6506.
18. J. Contreras-García, E. R. Johnson, S. Keinan, R. Chaudret, J.-P. Piquemal, D. N. Beratan and W. Yang, NCIPILOT: A Program for Plotting Noncovalent Interaction Regions, *J. Chem. Theor. Comput.*, 2011, **7**, 625-632.
19. T. A. Keith, AIMAll (Version 19.02.13).*Journal*, 2019.
20. L. E. Zelenkov, D. M. Ivanov, E. K. Sadykov, N. A. Bokach, B. Galmés, A. Frontera and V. Y. Kukushkin, Semicoordination Bond Breaking and Halogen Bond Making Change the Supramolecular Architecture of Metal-Containing Aggregates, *Crystal Growth & Design*, 2020, DOI: 10.1021/acs.cgd.0c00999.
21. J. Zhang, libreta: Computerized Optimization and Code Synthesis for Electron Repulsion Integral Evaluation, *Journal of Chemical Theory and Computation*, 2018, **14**, 572-587.
22. T. Lu and F. Chen, Multiwfn: A multifunctional wavefunction analyzer, *Journal of Computational Chemistry*, 2012, **33**, 580-592.
23. F. Weinhold and C. R. Landis, *Discovering Chemistry With Natural Bond Orbitals*, John Wiley & Sons, Hoboken, NJ, 2012.

24. M. J. Frisch, G. W. Trucks, H. B. Schlegel, G. E. Scuseria, M. A. Robb, J. R. Cheeseman, G. Scalmani, V. Barone, G. A. Petersson, H. Nakatsuji, X. Li, M. Caricato, A. V. Marenich, J. Bloino, B. G. Janesko, R. Gomperts, B. Mennucci, H. P. Hratchian, J. V. Ortiz, A. F. Izmaylov, J. L. Sonnenberg, D. Williams-Young, F. Ding, F. Lipparini, F. Egidi, J. Goings, B. Peng, A. Petrone, T. Henderson, D. Ranasinghe, V. G. Zakrzewski, J. Gao, N. Rega, G. Zheng, W. Liang, M. Hada, M. Ehara, K. Toyota, R. Fukuda, J. Hasegawa, M. Ishida, T. Nakajima, Y. Honda, O. Kitao, H. Nakai, T. Vreven, K. Throssell, J. A. Montgomery, Jr., J. E. Peralta, F. Ogliaro, M. J. Bearpark, J. J. Heyd, E. N. Brothers, K. N. Kudin, V. N. Staroverov, T. A. Keith, R. Kobayashi, J. Normand, K. Raghavachari, A. P. Rendell, J. C. Burant, S. S. Iyengar, J. Tomasi, M. Cossi, J. M. Millam, M. Klene, C. Adamo, R. Cammi, J. W. Ochterski, R. L. Martin, K. Morokuma, O. Farkas, J. B. Foresman and D. J. Fox, Gaussian 16, Revision C.01. *Journal*, 2016.
25. H. Graeme, Metal-dithiocarbamate complexes: chemistry and biological activity, *Mini-Reviews in Medicinal Chemistry*, 2012, **12**, 1202-1215.
26. D. Cen, D. Brayton, B. Shahandeh, F. L. Meyskens and P. J. Farmer, Disulfiram Facilitates Intracellular Cu Uptake and Induces Apoptosis in Human Melanoma Cells, *Journal of Medicinal Chemistry*, 2004, **47**, 6914-6920.
27. D. Chen, Q. C. Cui, H. Yang and Q. P. Dou, Disulfiram, a Clinically Used Anti-Alcoholism Drug and Copper-Binding Agent, Induces Apoptotic Cell Death in Breast Cancer Cultures and Xenografts via Inhibition of the Proteasome Activity, *Cancer Research*, 2006, **66**, 10425.
28. B. Cvek, V. Milacic, J. Taraba and Q. P. Dou, Ni(II), Cu(II), and Zn(II) Diethyldithiocarbamate Complexes Show Various Activities Against the Proteasome in Breast Cancer Cells, *Journal of Medicinal Chemistry*, 2008, **51**, 6256-6258.
29. S. Zdenek and C. Boris, Diethyldithiocarbamate complex with copper: the mechanism of action in cancer cells, *Mini-Reviews in Medicinal Chemistry*, 2012, **12**, 1184-1192.
30. R. Safi, E. R. Nelson, S. K. Chitneni, K. J. Franz, D. J. George, M. R. Zalutsky and D. P. McDonnell, Copper Signaling Axis as a Target for Prostate Cancer Therapeutics, *Cancer Research*, 2014, **74**, 5819.
31. Z. Skrott, M. Mistrik, K. K. Andersen, S. Friis, D. Majera, J. Gursky, T. Ozdian, J. Bartkova, Z. Turi, P. Moudry, M. Kraus, M. Michalova, J. Vaclavkova, P. Dzubak, I. Vrobel, P. Pouckova, J. Sedlacek, A. Mikloovicova, A. Kutt, J. Li, J. Mattova, C. Driessen, Q. P. Dou, J. Olsen, M. Hajduch, B. Cvek, R. J. Deshaies and J. Bartek, Alcohol-abuse drug disulfiram targets cancer via p97 segregase adaptor NPL4, *Nature*, 2017, **552**, 194.
32. D. Chen, F. Peng, Q. C. Cui, K. G. Daniel, S. Orlu, J. Liu and Q. P. Dou, INHIBITION OF PROSTATE CANCER CELLULAR PROTEASOME ACTIVITY BY A PYRROLIDINE DITHIOCARBAMATE-COPPER COMPLEX IS ASSOCIATED WITH SUPPRESSION OF PROLIFERATION AND INDUCTION OF APOPTOSIS, *Frontiers in Bioscience*, 2005, **10**, 2932-2939.
33. K. G. Daniel, D. Chen, S. Orlu, Q. C. Cui, F. R. Miller and Q. P. Dou, Clioquinol and pyrrolidine dithiocarbamate complex with copper to form proteasome inhibitors and apoptosis inducers in human breast cancer cells, *Breast Cancer Research*, 2005, **7**, R897.
34. V. Milacic, D. Chen, L. Giovagnini, A. Diez, D. Fregona and Q. P. Dou, Pyrrolidine dithiocarbamate-zinc(II) and -copper(II) complexes induce apoptosis in tumor cells by inhibiting the proteasomal activity, *Toxicology and Applied Pharmacology*, 2008, **231**, 24-33.
35. L. Giovagnini, S. Sitran, M. Montopoli, L. Caparrotta, M. Corsini, C. Rosani, P. Zanello, Q. P. Dou and D. Fregona, Chemical and Biological Profiles of Novel Copper(II) Complexes Containing S-Donor Ligands for the Treatment of Cancer, *Inorganic Chemistry*, 2008, **47**, 6336-6343.
36. F. P. Andrew and P. A. Ajibade, Synthesis, characterization and anticancer studies of bis(1-phenylpiperazine dithiocarbamato) Cu(II), Zn(II) and Pt(II) complexes: Crystal structures of 1-phenylpiperazine dithiocarbamato-S,S' zinc(II) and Pt(II), *Journal of Molecular Structure*, 2018, **1170**, 24-29.
37. F. P. Andrew and P. A. Ajibade, Synthesis, characterization and anticancer studies of bis-(N-methyl-1-phenyldithiocarbamato) Cu(II), Zn(II), and Pt(II) complexes: single crystal X-ray structure of the copper complex, *Journal of Coordination Chemistry*, 2018, **71**, 2776-2786.

38. M. K. Amir, S. Z. Khan, F. Hayat, A. Hassan, I. S. Butler and R. Ziaur, Anticancer activity, DNA-binding and DNA-denaturing aptitude of palladium(II) dithiocarbamates, *Inorganica Chimica Acta*, 2016, **451**, 31-40.
39. A. T. Odularu and P. A. Ajibade, Dithiocarbamates: Challenges, Control, and Approaches to Excellent Yield, Characterization, and Their Biological Applications, *Bioinorganic Chemistry and Applications*, 2019, **2019**, 15.
40. S. A. Hosseini, M. Eslami Moghadam, M. Saeidifar and A. A. Saboury, Biological effect and molecular docking of anticancer palladium and platinum complexes with morpholine dithiocarbamate on human serum albumin as a blood carrier protein, *Canadian Journal of Physiology and Pharmacology*, 2018, **96**, 1276-1285.
41. L. Marcheselli, C. Preti, M. Tagliazucchi, V. Cherchi, L. Sindellari, A. Furlani, A. Papaioannou and V. Scarcia, Synthesis, characterization and evaluation of biological activity of palladium (II) and platinum (II) complexes with dithiocarbamic acids and their derivatives as ligands, *European Journal of Medicinal Chemistry*, 1993, **28**, 347-352.
42. M. H. Lim and S. J. Lippard, Fluorescent Nitric Oxide Detection by Copper Complexes Bearing Anthracenyl and Dansyl Fluorophore Ligands, *Inorganic Chemistry*, 2006, **45**, 8980-8989.
43. P. Nath, M. K. Bharty, S. K. Kushawaha and B. Maiti, Synthesis, spectral, structural, photoluminescence, thermal and DFT studies of phenylmercury(II) and Ni(II) complexes of 3-methoxycarbonyl-piperidine-1-carbodithioate, *Polyhedron*, 2018, **151**, 503-509.
44. S. Poirier, E. Tailleur, H. Lynn and C. Reber, Characterization of Pd···H–C interactions in bis-dimethylidithiocarbamate palladium(ii) and its deuterated analog by luminescence spectroscopy at variable pressure, *Dalton Transactions*, 2016, **45**, 10883-10886.
45. C. Genre, G. Levasseur-Thériault and C. Reber, Emitting-state properties of square-planar dithiocarbamate complexes of palladium(II) and platinum(II) probed by pressure-dependent luminescence spectroscopy, *Canadian Journal of Chemistry*, 2009, **87**, 1625-1635.
46. A. Kumar, R. Chauhan, K. C. Molloy, G. Kociok-Köhn, L. Bahadur and N. Singh, Synthesis, Structure and Light-Harvesting Properties of Some New Transition-Metal Dithiocarbamates Involving Ferrocene, *Chemistry – A European Journal*, 2010, **16**, 4307-4314.
47. V. Singh, R. Chauhan, A. N. Gupta, V. Kumar, M. G. B. Drew, L. Bahadur and N. Singh, Photosensitizing activity of ferrocenyl bearing Ni(ii) and Cu(ii) dithiocarbamates in dye sensitized TiO<sub>2</sub> solar cells, *Dalton Transactions*, 2014, **43**, 4752-4761.
48. G. Gurumoorthy, S. Thirumaran and S. Ciattini, Synthesis and characterization of copper(II) dithiocarbamate complexes involving pyrrole and ferrocenyl moieties and their utility for sensing anions and preparation of copper sulfide and copper–iron sulfide nanoparticles, *Applied Organometallic Chemistry*, 2018, **32**, e4363.
49. G. I. Dzhardimalieva and I. E. Uflyand, Chalcogen-containing metal chelates as single-source precursors of nanostructured materials: recent advances and future development, *Journal of Coordination Chemistry*, 2019, **72**, 1425-1465.
50. E. Sathiyaraj, G. Gurumoorthy and S. Thirumaran, Nickel(ii) dithiocarbamate complexes containing the pyrrole moiety for sensing anions and synthesis of nickel sulfide and nickel oxide nanoparticles, *New Journal of Chemistry*, 2015, **39**, 5336-5349.
51. N. Hollingsworth, A. Roffey, H.-U. Islam, M. Mercy, A. Roldan, W. Bras, M. Wolthers, C. R. A. Catlow, G. Sankar, G. Hogarth and N. H. de Leeuw, Active Nature of Primary Amines during Thermal Decomposition of Nickel Dithiocarbamates to Nickel Sulfide Nanoparticles, *Chemistry of Materials*, 2014, **26**, 6281-6292.
52. R. Nomura, K. Miyawaki, T. Toyosaki and H. Matsuda, Preparation of copper sulfide thin layers by a single-source MOCVD process, *Chemical Vapor Deposition*, 1996, **2**, 174-179.
53. P. O'Brien and J. Waters, Deposition of Ni and Pd Sulfide Thin Films via Aerosol-Assisted CVD, *Chemical Vapor Deposition*, 2006, **12**, 620-626.
54. A. Birri, B. Harvey, G. Hogarth, E. Subasi and F. Uğur, Allyl palladium dithiocarbamates and related dithiolate complexes as precursors to palladium sulfides, *Journal of Organometallic Chemistry*, 2007, **692**, 2448-2455.

55. M. A. Ehsan, H. N. Ming, V. McKee, T. A. N. Peiris, U. Wijayantha-Kahagala-Gamage, Z. Arifin and M. Mazhar, Vysotskite structured photoactive palladium sulphide thin films from dithiocarbamate derivatives, *New Journal of Chemistry*, 2014, **38**, 4083-4091.
56. A. Angeloski, M. B. Cortie, J. A. Scott, D. M. Bordin and A. M. McDonagh, Conversion of single crystals of a nickel(II) dithiocarbamate complex to nickel sulfide crystals, *Inorganica Chimica Acta*, 2019, **487**, 228-233.
57. K. Nakatani, K. Himoto, Y. Kono, Y. Nakahashi, H. Anma, T. Okubo, M. Maekawa and T. Kuroda-Sowa, Synthesis, Crystal Structure, and Electroconducting Properties of a 1D Mixed-Valence Cu(I)-Cu(II) Coordination Polymer with a Dicyclohexyl Dithiocarbamate Ligand, *Crystals*, 2015, **5**, 215-225.
58. K. Himoto, S. Suzuki, T. Okubo, M. Maekawa and T. Kuroda-Sowa, A new semiconducting 1D Cu(i)-Cu(ii) mixed-valence coordination polymer with Cu(ii) dimethylpiperidine-dithiocarbamate and a tetranuclear Cu(i)-Br cluster unit, *New Journal of Chemistry*, 2018, **42**, 3995-3998.
59. K. K. Ho, U. Takashi, O. Takashi, H. Shinya, A. Haruho, K. Kazuya, S. Tetsuya, F. Jyunji, M. Masahiko and K.-S. Takayoshi, Synthesis and Conducting Properties of a New Mixed-valence Cu(I)-Cu(II) 1-D Coordination Polymer Bridged by Morpholine Dithiocarbamate, *Chemistry Letters*, 2011, **40**, 1184-1186.
60. T. Okubo, R. Kawajiri, T. Mitani and T. Shimoda, A Mixed-Valence Coordination Polymer Featuring Two-Dimensional Ferroelectric Order: {[Cul4Cull(Et<sub>2</sub>dtc)2Cl<sub>3</sub>][Cull(Et<sub>2</sub>dtc)2]2(FeCl<sub>4</sub>)<sub>n</sub>} (Et<sub>2</sub>dtc- = diethyldithiocarbamate), *Journal of the American Chemical Society*, 2005, **127**, 17598-17599.
61. T. Okubo, N. Tanaka, K. H. Kim, H. Yone, M. Maekawa and T. Kuroda-Sowa, Magnetic and Conducting Properties of New Halide-Bridged Mixed-Valence Cul-Cull 1D Coordination Polymers Including a Hexamethylene Dithiocarbamate Ligand, *Inorganic Chemistry*, 2010, **49**, 3700-3702.
62. T. Okubo, N. Tanaka, K. H. Kim, H. Anma, S. Seki, A. Saeki, M. Maekawa and T. Kuroda-Sowa, Crystal structure and carrier transport properties of a new 3D mixed-valence Cu(i)-Cu(ii) coordination polymer including pyrrolidine dithiocarbamate ligand, *Dalton Transactions*, 2011, **40**, 2218-2224.
63. T. Okubo, H. Anma, N. Tanaka, K. Himoto, S. Seki, A. Saeki, M. Maekawa and T. Kuroda-Sowa, Crystal structure and carrier transport properties of a new semiconducting 2D coordination polymer with a 3,5-dimethylpiperidine dithiocarbamate ligand, *Chemical Communications*, 2013, **49**, 4316-4318.
64. T. Okubo, H. Anma, Y. Nakahashi, M. Maekawa and T. Kuroda-Sowa, New one-dimensional mixed-valence coordination polymers including an iodine-bridged pentanuclear copper(I) cluster unit, *Polyhedron*, 2014, **69**, 103-109.
65. N. Tanaka, T. Okubo, H. Anma, K. H. Kim, Y. Inuzuka, M. Maekawa and T. Kuroda-Sowa, Halido-Bridged 1D Mixed-Valence Cul-Cull Coordination Polymers Bearing a Piperidine-1-carbodithioato Ligand: Crystal Structure, Magnetic and Conductive Properties, and Application in Dye-Sensitized Solar Cells, *European Journal of Inorganic Chemistry*, 2013, **2013**, 3384-3391.
66. R. M. Golding, A. D. Rae and L. Sulligoi, New series of polynuclear copper dithiocarbamate-copper halide polymers, *Inorganic Chemistry*, 1974, **13**, 2499-2504.
67. C. Wang, J. Niu, J. Li and X. Ma, Synthesis, structures and properties of three copper complexes with dibutylidithiocarbamate ligand, *Journal of Molecular Structure*, 2017, **1135**, 75-81.
68. L.-Q. Fan and X.-T. Zhu, Syntheses and crystal structures of two heterometallic iodoplumbates containing mixed-valence copper(I/II), *Acta Crystallographica Section C*, 2017, **73**, 1098-1103.
69. T. Okubo, N. Tanaka, H. Anma, K. H. Kim, M. Maekawa and T. Kuroda-Sowa, Dye-sensitized Solar Cells with New One-Dimensional Halide-Bridged Cu(I)-Ni(II) Heterometal Coordination Polymers Containing Hexamethylene Dithiocarbamate Ligand, *Polymers*, 2012, **4**, 1613-1626.
70. K. Himoto, T. Horii, S. Oda, S. Suzuki, K. Sugimoto, T. Okubo, M. Maekawa and T. Kuroda-Sowa, Crystal structure of a new mixed-metal coordination polymer consisting of Ni<sup>II</sup> piperidine-dithiocarbamate and pentanuclear Cul-I cluster units, *Acta Crystallographica Section E*, 2018, **74**, 233-236.

71. M. Ebihara, K. Tokoro, M. Maeda, M. Ogami, K. Imaeda, K. Sakurai, H. Masuda and T. Kawamura, Bonding interaction between Group 10 and 11 metals. Synthesis, structure and properties of  $[M_3(S_2CNR_2)6M'_{2+}]_{2+}$  ( $M = Pt$  or  $Pd$ ;  $M' = Ag$  or  $Cu$ ;  $R = Et$ ,  $Pri$ ,  $Prn$ ,  $Bun$  or  $C_6H_{11}$ ), *Journal of the Chemical Society, Dalton Transactions*, 1994, DOI: 10.1039/DT9940003621, 3621-3635.
72. K. Tokoro, M. Ebihara and T. Kawamura,  $(CuX)_n$  Helical Chains in  $[Pt(S_2CNEt_2)_2Cu_2X_2]$  ( $X = Br$ ,  $Cl$ ), *Acta Crystallographica Section C*, 1995, **51**, 2010-2013.
73. E. Masahiro, S. Kenji, K. Takashi, K. Hiroaki, M. Hideki and T. Tooru, Covalent Bonding of Two  $Ag(I)$  Atoms to a Square-Planar  $Pt(II)$  Atom in  $[Pt_3(S_2CNEt_2)_6Ag_2](ClO_4)_2$ , *Chemistry Letters*, 1990, **19**, 415-418.
74. T. Okubo, H. Kuwamoto, K. H. Kim, S. Hayami, A. Yamano, M. Shiro, M. Maekawa and T. Kuroda-Sowa, Intervalence Charge-Transfer System by 1D Assembly of New Mixed-Valence Octanuclear  $CuI/CuII/CuIII$  Cluster Units, *Inorganic Chemistry*, 2011, **50**, 2708-2710.
75. T. Okubo, H. Anma, M. Maekawa and T. Kuroda-Sowa, Tris( $\mu$ )-4-azepane-1-carbodithioato)bis( $\mu$ )-3-azepane-1-carbodithioato)- $\mu$ -9-bromido-tetra- $\mu$ -2-bromido-octacopper(I)copper(II), *Acta Crystallographica Section E*, 2013, **69**, m275-m276.
76. M. Sokolov, H. Imoto and T. Saito, Ligand transfer between hard and soft metal centres. Synthesis and X-ray characterisation of a new trinuclear  $Pd(II)$  dithiocarbamate  $Pd_3(Et_2NCS_2)_4Cl_2$ , *Inorganic Chemistry Communications*, 1999, **2**, 422-423.
77. A. J. Blake, P. Kathirgamanathan and M. J. Toohey, Structures of a novel trinuclear palladium(II) dithiocarbamate complex and of bis(diethyldithiocarbamato)dibromopalladium(IV), *Inorganica Chimica Acta*, 2000, **303**, 137-139.
78. M. Ebihara, K. Tokoro, K. Imaeda, K. Sakurai, H. Masuda and T. Kawamura, Complexes of silver(I) with bis(dialkyldithiocarbamato)platinum(II) as ligand: synthesis and structures of  $[Pt_3(S_2CNPri_2)_6Ag_2](BF_4)_2$  and  $[Pt_3(S_2CNBun_2)_6Ag_2](ClO_4)_2$ , *Journal of the Chemical Society, Chemical Communications*, 1992, DOI: 10.1039/C39920001591, 1591-1592.
79. S. Poirier, P. Guionneau, D. Luneau and C. Reber, Why do the luminescence maxima of isostructural palladium(II) and platinum(II) complexes shift in opposite directions?, *Canadian Journal of Chemistry*, 2014, **92**, 958-965.
80. S. Poirier, R. J. Roberts, D. Le, D. B. Leznoff and C. Reber, Interpreting Effects of Structure Variations Induced by Temperature and Pressure on Luminescence Spectra of Platinum(II) Bis(dithiocarbamate) Compounds, *Inorganic Chemistry*, 2015, **54**, 3728-3735.
81. S. Poirier, F. Rahmani and C. Reber, Large d-d luminescence energy variations in square-planar bis(dithiocarbamate) platinum(ii) and palladium(ii) complexes with near-identical MS4 motifs: a variable-pressure study, *Dalton Transactions*, 2017, **46**, 5279-5287.
82. P. D. Beer, N. Berry, M. G. B. Drew, O. D. Fox, M. E. Padilla-Tosta and S. Patell, Self-assembled dithiocarbamate-copper(ii) macrocycles for electrochemical anion recognition, *Chemical Communications*, 2001, DOI: 10.1039/B007296F, 199-200.
83. C. Yuan, B. Liu, F. Liu, M.-Y. Han and Z. Zhang, Fluorescence "Turn On" Detection of Mercuric Ion Based on Bis(dithiocarbamato)copper(II) Complex Functionalized Carbon Nanodots, *Analytical Chemistry*, 2014, **86**, 1123-1130.
84. A. V. Rozhkov, A. S. Novikov, D. M. Ivanov, D. S. Bolotin, N. A. Bokach and V. Y. Kukushkin, Structure-Directing Weak Interactions with 1,4-Diodotetrafluorobenzene Convert One-Dimensional Arrays of  $[M^{II}(acac)_2]$  Species into Three-Dimensional Networks, *Cryst. Growth Des.*, 2018, **18**, 3626-3636.
85. O. I. Kucheriv, S. I. Shylin, V. Ksenofontov, S. Dechert, M. Haukka, I. O. Fritsky and I. y. A. Gural'skiy, Spin Crossover in  $Fe(II)-M(II)$  Cyanoheterobimetallic Frameworks ( $M = Ni$ ,  $Pd$ ,  $Pt$ ) with 2-Substituted Pyrazines, *Inorganic Chemistry*, 2016, **55**, 4906-4914.
86. Z. M. Bikbaeva, D. M. Ivanov, A. S. Novikov, I. V. Ananyev, N. A. Bokach and V. Y. Kukushkin, Electrophilic-Nucleophilic Dualism of Nickel(II) toward  $Ni \cdots I$  Noncovalent Interactions: Semicoordination of Iodine Centers via Electron Belt and Halogen Bonding via  $\sigma$ -Hole, *Inorganic Chemistry*, 2017, **56**, 13562-13578.
87. Y. Yamashina, Y. Kataoka and Y. Ura, Inclusion of an Iodine Molecule in a Tiara-Like Octanuclear Palladium Thiolate Complex, *European Journal of Inorganic Chemistry*, 2014, **2014**, 4073-4078.

88. S. V. Baykov, U. Dabranskaya, D. M. Ivanov, A. S. Novikov and V. P. Boyarskiy, Pt/Pd and I/Br Isostructural Exchange Provides Formation of C—I···Pd, C—Br···Pt, and C—Br···Pd Metal-Involving Halogen Bonding, *Crystal Growth & Design*, 2018, **18**, 5973-5980.
89. E. A. Katlenok, A. V. Rozhkov, O. V. Levin, M. Haukka, M. L. Kuznetsov and V. Y. Kukushkin, Halogen Bonding Involving Palladium(II) as an XB Acceptor, *Crystal Growth & Design*, 2020, DOI: 10.1021/acs.cgd.0c01474.
90. L. S. v. Chrzanowski, M. Lutz, A. L. Spek, B. M. J. M. Suijkerbuijk and R. J. M. Klein Gebbink, {2,6-Bis[(dimethylamino-[kappa]N)methyl]-4-[(2,5-dioxo-1-pyrrolidinyl)oxy]carbonyl}phenyl-[kappa]C1(diiodine)iodidoplatinum(II) dichloromethane hemisolvate, *Acta Crystallographica Section E*, 2007, **63**, m1223-m1225.
91. R. A. Gossage, A. D. Ryabov, A. L. Spek, D. J. Stufkens, J. A. M. van Beek, R. van Eldik and G. van Koten, Models for the Initial Stages of Oxidative Addition. Synthesis, Characterization, and Mechanistic Investigation of  $\eta^1$ -I2 Organometallic “Pincer” Complexes of Platinum. X-ray Crystal Structures of [PtI(C6H3{CH2NMe2}2-2,6)( $\eta^1$ -I2)] and exo-meso-[Pt( $\eta^1$ -I3)( $\eta^1$ -I2)(C6H3{CH2N(t-Bu)Me}2-2,6)], *Journal of the American Chemical Society*, 1999, **121**, 2488-2497.
92. J. A. M. van Beek, G. van Koten, G. P. C. M. Dekker, E. Wissing, M. C. Zoutberg and C. H. Stam, Synthesis and reactivity towards diiodine of palladium(II) and platinum(II) complexes with non-cyclic and cyclic ligands (C6H3{CH2NR1R2}2-2,6)-. End-on diiodine-platinum(II) bonding in macrocyclic [PtI(C6H3{CH2NMe(CH2)7MeNCH2}-2,6)( $\eta^1$ -I2)], *Journal of Organometallic Chemistry*, 1990, **394**, 659-678.
93. E. A. Katlenok, M. Haukka, O. V. Levin, A. Frontera and V. Y. Kukushkin, Supramolecular Assembly of Metal Complexes by (Aryl)I···d [PtII] Halogen Bonds, *Chemistry – A European Journal*, 2020, **26**, 7692-7701.
94. D. M. Ivanov, A. S. Novikov, I. V. Ananyev, Y. V. Kirina and V. Y. Kukushkin, Halogen bonding between metal centers and halocarbons, *Chemical Communications*, 2016, **52**, 5565-5568.
95. A. V. Rozhkov, D. M. Ivanov, A. S. Novikov, I. V. Ananyev, N. A. Bokach and V. Y. Kukushkin, Metal-involving halogen bond Ar—I···[dz2PtII] in a platinum acetylacetone complex, *CrystEngComm*, 2020, **22**, 554-563.
96. N. D. Yordanov and D. Shopov, EPR studies of dithiophosphate and dithiocarbamate complexes. III. Influence of axial ligands on the structure of copper(II) complexes, *Inorganica Chimica Acta*, 1971, **5**, 679-682.
97. D. V. Konarev, A. Y. Kovalevsky, S. S. Khasanov, G. Saito, D. V. Lopatin, A. V. Umrikhin, A. Otsuka and R. N. Lyubovskaya, Synthesis, Crystal Structures, Magnetic Properties and Photoconductivity of C60 and C70 Complexes with Metal Dialkyldithiocarbamates M(R2dtc)x, where M = CuI, Cul, AgI, ZnII, CdII, HgII, MnII, NiII, and PtII; R = Me, Et, and nPr, *European Journal of Inorganic Chemistry*, 2006, **2006**, 1881-1895.
98. D. V. Konarev, A. Y. Kovalevsky, D. V. Lopatin, A. V. Umrikhin, E. I. Yudanova, P. Coppens, R. N. Lyubovskaya and G. Saito, Synthesis, crystal structure and photoconductivity of the first [60]fullerene complex with metal diethyldithiocarbamate: {CuII(dedtc)2}2·C60, *Dalton Transactions*, 2005, DOI: 10.1039/B500314H, 1821-1825.
99. M. Bonamico, G. Dessy, A. Mugnoli, A. Vaciago and L. Zambonelli, Structural studies of metal dithiocarbamates. II. The crystal and molecular structure of copper diethyldithiocarbamate, *Acta Crystallographica*, 1965, **19**, 886-897.
100. B. H. O'Connor and E. N. Maslen, A second analysis of the crystal structure of copper(II) diethyldithiocarbamate, *Acta Crystallographica*, 1966, **21**, 828-830.
101. F. Jian, Z. Wang, Z. Bai, X. You, H.-K. Fun, K. Chinnakali and I. A. Razak, The crystal structure, equilibrium and spectroscopic studies of bis(dialkyldithiocarbamate) copper(II) complexes [Cu2(R2dtc)4] (dtc=dithiocarbamate), *Polyhedron*, 1999, **18**, 3401-3406.
102. S. K. Verma, R. Kadu and V. K. Singh, A Facile Synthesis, Crystallographic, Spectral, Thermal, and Electrochemical Investigations of Neutral [Cu2(Et2dtc)4] Dimer, *Synthesis and Reactivity in Inorganic, Metal-Organic, and Nano-Metal Chemistry*, 2014, **44**, 441-448.
103. P. W. G. Newman, C. L. Raston and A. H. White, Crystal structures of bis(pyrrolidonecarbodithioato)-nickel(II) and -copper(II), *Journal of the Chemical Society, Dalton Transactions*, 1973, DOI: 10.1039/DT9730001332, 1332-1335.

104. C. Raston and A. White, Crystal structure of Bis(N,N-diisobutyldithiocarbamato)nickel(II), *Australian Journal of Chemistry*, 1976, **29**, 523-529.
105. A. Husain, S. A. A. Nami, S. P. Singh, M. Oves and K. S. Siddiqi, Anagostic interactions, revisiting the crystal structure of nickel dithiocarbamate complex and its antibacterial and antifungal studies, *Polyhedron*, 2011, **30**, 33-40.
106. G. Rajput, V. Singh, A. N. Gupta, M. K. Yadav, V. Kumar, S. K. Singh, A. Prasad, M. G. B. Drew and N. Singh, Unusual C–H…Ni anagostic interactions in new homoleptic Ni(ii) dithio complexes, *CrystEngComm*, 2013, **15**, 4676-4683.
107. S. K. Singh, M. G. B. Drew and N. Singh, Self assembly of homoleptic Ni(ii) dithiocarbamates and dithiocarbimates via Ni…H–C anagostic and C–H…π (chelate) interactions, *CrystEngComm*, 2013, **15**, 10255-10265.
108. A. N. Gupta, V. Kumar, V. Singh, K. K. Manar, M. G. B. Drew and N. Singh, Intermolecular anagostic interactions in group 10 metal dithiocarbamates, *CrystEngComm*, 2014, **16**, 9299-9307.
109. M. K. Yadav, G. Rajput, L. B. Prasad, M. G. B. Drew and N. Singh, Rare intermolecular M…H–C anagostic interactions in homoleptic Ni(ii)–Pd(ii) dithiocarbamate complexes, *New Journal of Chemistry*, 2015, **39**, 5493-5499.
110. J. A. M. Van Beek, G. Van Koten, W. J. J. Smeets and A. L. Spek, Model for the initial stage in the oxidative addition of I<sub>2</sub> to organoplatinum(II) compounds. X-ray structure of square-pyramidal [Pt<sup>II</sup>{C<sub>6</sub>H<sub>3</sub>(CH<sub>2</sub>NMe<sub>2</sub>)<sub>2</sub>-o,o'}(.eta.1-I<sub>2</sub>)] containing a linear Pt–I–I arrangement, *Journal of the American Chemical Society*, 1986, **108**, 5010-5011.
111. L. Koskinen, P. Hirva, E. Kalenius, S. Jääskeläinen, K. Rissanen and M. Haukka, Halogen bonds with coordinative nature: halogen bonding in a S–I+–S iodonium complex, *CrystEngComm*, 2015, **17**, 1231-1236.